

Ultrasonic velocity in the mixed state of Nb-26-at. % Hf

F. P. Missell

Instituto de Física, Universidade de São Paulo, Caixa Postal 20516 São Paulo, São Paulo, Brazil

(Received 7 July 1978)

The magnetic-field-dependent change in the ultrasonic velocity was measured in the mixed state of Nb-26-at. % Hf at $T = 4.14$ K, using shear and longitudinal waves with frequencies 5–30 MHz. The results are compared with phenomenological models in which the flux-flow resistivity is used as an effective resistivity in the Alpher-Rubin theory.

Previously¹ we presented measurements of the attenuation of longitudinal and transverse ultrasonic waves in the mixed state of Nb-26-at. % Hf. The results were compared with a phenomenological model^{2,3} for the attenuation in the mixed state which was proposed by Shapira and Neuringer (SN). These authors used a simplified form for the ac resistivity associated with flux-line motion⁴ as an effective resistivity in the Alpher-Rubin (AR) theory⁵ to obtain an expression for the attenuation in the mixed state. We also modified¹ the SN model by using Thompson's result for the flux-flow resistivity in the absence of pinning forces⁶ as an effective resistivity in the AR theory. The revised theory improved agreement with experimental data for the H dependence of the attenuation for high frequencies where pinning forces could be neglected. Here we present measurements of the H -dependent sound-velocity changes for longitudinal and transverse waves in the mixed state of Nb-26-at. % Hf and compare these with both the SN model and the revised theory.

The H -dependent change in the sound velocity, for shear waves with wave vector $\vec{q} \parallel \vec{H}$ and longitudinal waves with $\vec{q} \perp \vec{H}$, is

$$(\Delta V/V)_n \equiv [V(H) - V(0)]/V(0) = \mu H^2 / 8\pi d V^2 (1 + \beta^2), \quad (1)$$

where d is the density of the sample, V is the zero-field sound velocity (V_L for longitudinal waves and V_S for shear waves), and μ is the permeability. We define $\beta = c^2 \omega \rho_n / 4\pi \mu V^2$, where ω is the ultrasonic frequency and ρ_n is the normal-state resistivity. Equation (1) is the classical result of the AR theory and has been extensively verified for normal metals with low resistivities.⁷

The main assumption of the SN model is that the sound velocity in the *mixed state* can be obtained from the AR theory by replacing the normal electrical resistivity with the mixed-state resistivity for a frequency ω equal to that of the sound frequency. Employing an effective ac resistivity for the mixed state,⁴ SN obtained an expression for the H -dependent velocity change^{2,3}:

$$\left(\frac{\Delta V}{V}\right)_s = \left(\frac{\mu H^2}{8\pi d V^2}\right) \left(\frac{(1+r^2+r\beta_f)(1+r^2)}{(1+r^2+r\beta_f)^2 + \beta_f^2}\right). \quad (2)$$

This result is for longitudinal waves with $\vec{q} \perp \vec{H}$ and shear waves with $\vec{q} \parallel \vec{H}$ and should be valid for $H_{c2} > H \gg H_{c1}$. In Eq. (2), the parameter β_f is obtained from β by replacing the normal resistivity ρ_n by the flow resistivity $\rho_f = \rho_n H / H_{c2}^*(0)$, where $H_{c2}^*(0)$ is the upper critical field in the absence of paramagnetic limiting. We also define $r = \omega_0 / \omega$, where ω_0 is a frequency characteristic of flux-line motion known as the "depinning frequency."^{2,3} In comparing our experimental results to this model, it is convenient to consider the quantity $(\Delta V/V)_s / (\Delta V/V)_n$, obtained by dividing Eq. (2) by Eq. (1):

$$\frac{(\Delta V/V)_s}{(\Delta V/V)_n} = \frac{(1+r^2+r\beta_f)(1+r^2)(1+\beta^2)}{(1+r^2+r\beta_f)^2 + \beta_f^2}. \quad (3)$$

All quantities appearing in the right-hand side of Eq. (3) were determined experimentally¹ and, therefore, this model involves no adjustable parameters.

The attenuation data of Ref. 1 were also compared with a revised theory in which the effective resistivity in the AR theory was taken to be Thompson's result,⁶ obtained from a solution to the time-dependent Ginzburg-Landau equation. This result, which, in the dc limit, gives the dc flux-flow resistivity, should be valid only for frequencies sufficiently high that pinning effects may be neglected ($\omega \gg \omega_0$). The revised theory improved agreement with experimental data for the H dependence of the high-frequency attenuation, and it also gave a good account of the attenuation data at much lower frequencies where pinning effects are important. Thus it seemed desirable to compare the present *velocity* data with the revised theory, even though the estimated values¹ of ω_0 are comparable to the frequencies used in these experiments. Thompson's result for the flux-flow resistivity has the form $\rho = \rho_n / g$ where $g = 1 + \gamma(1 - H/H_{c2})$ and the quantity γ , defined in Eq. (16) of Ref. 1, is constant for

a fixed temperature. Using this result, we have

$$(\Delta V/V)_s/(\Delta V/V)_n = g^2(1+\beta^2)/(g^2+\beta^2). \quad (4)$$

In Ref. 1 we found that $\gamma = 3.2$ reproduced the slope of high-frequency attenuation data for $T = 4.14$ K and was in order-of-magnitude agreement with our *a priori* estimate of this quantity.

Measurements of the sound velocity at $T = 4.14$ K for shear and longitudinal waves with frequencies 5–30 MHz were made as a function of magnetic field in the sample of Nb–26-at.% Hf used previously.¹ The system for sound-velocity measurements, which employs a modified pulse-superposition method,^{8,9} had a resolution of better than 1 ppm. For shear waves with $\vec{q} \perp \vec{H}$ and longitudinal waves with $\vec{q} \parallel \vec{H}$, $\Delta V/V$ was independent of H to within this resolution. The physical properties of our Nb–26-at.% Hf sample were discussed extensively in Ref. 1.

In Fig. 1 we show $\Delta V/V$ for 10-MHz shear waves with $\vec{q} \parallel \vec{H}$ at $T = 4.14$ K. The dashed curve, calculated from Eq. (1) using the measured values of d , V_s , and ρ_n , represents the AR theory and is in good agreement with the data for $H > H_{c2}$. For H just below H_{c2} we see a peak in $\Delta V/V$ that is associated with a peak in the critical current for fields just below H_{c2} (see Fig. 2 of Ref. 1). In a manner analogous to our treatment of attenuation,¹ we will compare the sound-velocity changes in the mixed state with $(\Delta V/V)_n$ the sound velocity changes that would have existed at temperature T and field H , had the material been normal. We calculate $(\Delta V/V)_n$ at fields $0.5 < H/H_{c2} < 1$ by extrapolating to lower fields the velocity changes measured at $H > H_{c2}$. In Fig. 1 we show this extrapolation for shear waves. The extrapolation is carried out by making a least-squares fit to the equation $\Delta V/V = mH^2$, where m is a constant. The measured velocity change in the mixed state is identified with $(\Delta V/V)_s$.

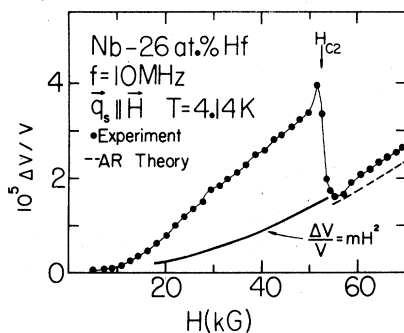


FIG. 1. Magnetic field variation of the ultrasonic velocity change $\Delta V/V$ for shear waves in Nb–26-at.% Hf.

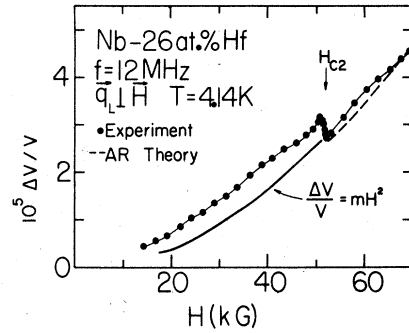


FIG. 2. Magnetic field variation of $\Delta V/V$ for longitudinal waves in Nb–26-at.% Hf.

In Fig. 2 we show $\Delta V/V$ for 12-MHz longitudinal waves with $\vec{q} \perp \vec{H}$ at $T = 4.14$ K. Again, the dashed curve represents the AR theory and is in good agreement with the data above H_{c2} . In Fig. 2 we also show the extrapolation to lower fields of velocity changes measured at $H > H_{c2}$. Here too we see a peak in $\Delta V/V$ just below H_{c2} , which can be associated with a peak in the critical current J_c for fields just below H_{c2} .

In Fig. 3 we show the normalized velocity $(\Delta V/V)_s/(\Delta V/V)_n$ as a function of H for the data of Fig. 2; the peak in the experimental data is clearly evident for $H \sim 51$ kG. The heavy solid curve of Fig. 3 (denoted SN theory) was calculated from Eq. (3) using the values of $\omega_0(H)$ from Fig. 2 of Ref. 1. These values of $\omega_0(H)$ were calculated from experimental values of J_c . The peak in the theoretical curve¹⁰ below H_{c2} confirms our previous identification of the similar peak in the experimental data with the peak in J_c . The SN model gives reasonable agreement with experimental values of $(\Delta V/V)_s/(\Delta V/V)_n$ for $H \sim 25$ –45 kG but tends to overestimate the value of this quantity

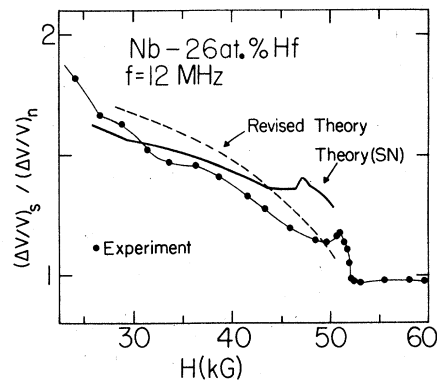


FIG. 3. Normalized sound-velocity change $(\Delta V/V)_s/(\Delta V/V)_n$ as a function of magnetic field for the 12-MHz longitudinal waves of Fig. 2.

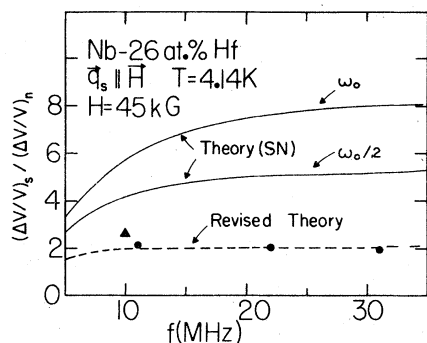


FIG. 4. Frequency dependence of $(\Delta V/V)_s/(\Delta V/V)_n$ for shear waves in Nb-26-at. % Hf.

near H_{c2} . This same problem was also noted for the high-frequency attenuation near H_{c2} and was one of the principal motivations for the revised theory. The dashed curve of Fig. 3 was calculated from Eq. (4) using $\gamma = 3.2$ and $H_{c2} = 51.9$ kG, values which were used in Ref. 1 to compare the revised model with the high-frequency attenuation data. Except for the peak¹¹ near H_{c2} , we see that the revised model gives a reasonable account of the form of $(\Delta V/V)_s/(\Delta V/V)_n$ for $(25 \text{ kG}) \lesssim H < H_{c2}$. In general, we find that both the SN and revised theories are in reasonably good agreement for $H \sim 25\text{--}45$ kG, for longitudinal waves in the frequency range of our experiments.

The differences between the two models become more apparent for shear waves. In Fig. 4 we show the frequency dependence of $(\Delta V/V)_s/(\Delta V/V)_n$ for shear waves with $\vec{q} \parallel \vec{H}$ at $T = 4.14$ K and for $H = 45$ kG. Using $\gamma = 3.2$ and $H_{c2} = 51.9$ kG in Eq. (4), the revised theory (dashed curve) is in good agreement with the experimental points (solid circles and triangle). The solid curves of Fig. 4 were calculated from Eq. (3) using ω_0 ($H = 45$ kG) (curve designated ω_0) and $\frac{1}{2}\omega_0$ ($H = 45$ kG) (curve designated $\omega_0/2$). According to the SN model, $(\Delta V/V)_s/(\Delta V/V)_n$ is quite sensitive to the value

of ω_0 , and tends to overestimate this quantity for any reasonable value of ω_0 . The best agreement between the data and Eq. (3) is obtained with $r = 0$ ($\omega_0 = 0$), in which case $(\Delta V/V)_s/(\Delta V/V)_n = (1 + \beta^2)/(1 + \beta_f^2)$ is, for example, $\sim 5\%$ above the dashed curve at 10 MHz. Since Eq. (2) for $(\Delta V/V)_s$ depends more heavily on the contribution of the *imaginary part* of the mixed-state resistivity $r\rho_n/(1+r^2)$, the difficulties of the SN model may reflect this fact. Indeed, previous experiments^{12,13} with shear waves ($\vec{q} \parallel \vec{H}$) in the mixed state of unannealed Nb-25-at. % Zr (for which $\omega_0 \gg \omega$) were shown to be in good agreement with Eq. (1) upon taking $\rho_n = 0$ ($\beta = 0$). This is essentially equivalent to making $r \gg 1$ ($\omega_0 \gg \omega$) in Eq. (2), a condition that was actually satisfied in those experiments. Thus, for the conditions of Refs. 12 and 13, the calculated contribution of the imaginary part of the mixed-state resistivity to $(\Delta V/V)_s$ is small and SN obtained agreement between their data and the model. Our experimental results may thus appear to favor Thompson's expression for the resistivity since the simple model used by SN seems to encounter difficulties when the imaginary part is large. However, Possin and Shepard¹⁴ actually measured the imaginary part of the mixed-state impedance and obtained good agreement with the simple model, and so the situation is more complicated. Additional theoretical work would be extremely useful in this area.

ACKNOWLEDGMENTS

I am pleased to acknowledge the financial support of Conselho Nacional de Desenvolvimento Científico e Tecnológico (CNPq) and Fundação de Amparo à Pesquisa do Estado de São Paulo (FAPESP). I acknowledge useful discussions with Y. Shapira and thank L. J. Neuringer for the sample used here. Technical discussions with J. M. V. Martins and N. Patel were most useful as was the technical assistance of S. Salem-Sugui, Jr.

¹F. P. Missell, N. F. Oliveira, Jr., and Y. Shapira, Phys. Rev. B **14**, 2255 (1976).

²Y. Shapira and L. J. Neuringer, Phys. Rev. **154**, 375 (1967).

³Y. Shapira, in *Physical Acoustics*, edited by W. P. Mason (Academic, New York, 1968), Vol. V., p. 1.

⁴J. I. Gittleman and B. Rosenblum, Phys. Rev. Lett. **16**, 734 (1966).

⁵R. A. Alpher and R. J. Rubin, J. Acoust. Soc. Am. **26**, 452 (1954).

⁶R. S. Thompson, Phys. Rev. B **1**, 327 (1970).

⁷G. A. Alers and P. A. Fleury, Phys. Rev. **129**, 2425 (1963).

⁸J. M. V. Martins and F. P. Missell, J. Phys. E **8**, 905 (1975).

⁹J. M. V. Martins, F. P. Missell, and J. R. Pereira, Phys. Rev. B **17**, 4633 (1978).

¹⁰In Fig. 3, the peak in the theoretical curve (SN) falls somewhat below the corresponding peak in the experimental curve. A similar discrepancy occurs in the case of the attenuation. (See Figs. 5 and 6 of Ref. 1.) Part of this discrepancy is almost certainly related to the criteria used to define J_c and H_{c2} in Ref. 1. On the other hand, the phenomenological model for the effective ac resistivity in the mixed state of Gittleman and Rosenblum is very simple and we cannot expect

its use in the AR theory to result in a detailed account of the *ultrasonic attenuation* near H_{c2} .

¹¹Of course, we do not expect the revised model to predict a peak near H_{c2} . The dashed curve of Fig. 3 was calculated using Thompson's result for the flux-flow resistivity in the *absence* of pinning forces (see Ref. 6) as an effective resistivity in the AR theory.

¹²Y. Shapira and L. J. Neuringer, Phys. Rev. Lett. 15, 724 (1965); 15, 873(E) (1965).

¹³L. J. Neuringer and Y. Shapira, Phys. Rev. 148, 231 (1966).

¹⁴G. E. Possin and K. W. Shepard, Phys. Rev. 171, 458 (1968).